Applied Engineering Letters Vol.8, No.3, 111-120 (2023) e-ISSN: 2466-4847

# ARTIFICIAL NEURAL NETWORK MODELING OF TRIBOLOGICAL PARAMETERS OPTIMIZATION OF AZ31-SiC METAL MATRIX COMPOSITE

UDC:620.178.16:004.8
Original scientific paper https://doi.org/10.18485/aeletters.2023.8.3.3

**Kothuri Chenchu Kishor Kumar[1*], Bandlamudi Raghu Kumar[2], Nalluri Mohan Rao[3]**

[1]Gudlavalleru Engineering College, Gudlavalleru-521 356, India
[2]Prasad V Potluri Siddhartha Institute of Technology, Vijayawada-520001, India
[3]Jawaharlal Nehru Technological University Kakinada, Kakinada-533003, India

**Abstract:**
This paper focuses on modeling the tribological properties of AZ31-SiC composite using an artificial neural network (ANN) fabricated through the stir casting method. The twenty-seven tests were performed with three loads (10 N, 15 N, and 20 N), three sliding speeds (0.5 m/s, 1.0 m/s, and 1.5 m/s), and three sliding distances (500 m, 750 m, and 1000 m) on wear testing machine and are used in the formation of training sets of ANN. Using the wear test data, Taguchi, Analysis of Variance (ANOVA), and regression analysis were carried out to determine the effect of the control parameters on the wear and coefficient of friction (COF). The experimental results demonstrate that the wear rate increases with an increase in load and distance and decreases with an increase in velocity. In addition, an alternative method is proposed to predict the wear and COF using ANN modeling with single and multi-hidden layer techniques. With good training, ANN gives accurate and close results to the experimental results. The results obtained using ANN modeling have a percentage of error of 4.71% and 5.79% for wear and COF respectively, when compared to experimental values. This prediction process saves time and costs for the manufacturer.

**ARTICLE HISTORY**
Received: 5 January 2023
Revised: 8 June 2023
Accepted: 2 July 2023
Published: 30 September 2023

**KEYWORDS**
AZ31 alloy, silicon carbide, wear parameters, optimization, artificial neural network, modeling

## 1. INTRODUCTION

Composite material is a mixture of two or more materials or phases of the same material, insoluble in one another, possessing properties that are superior to any of the component materials [1, 2]. The demand for magnesium alloys has been increasing due to their small weight and excellent cast-ability compared to aluminum alloys [3]. Nevertheless, magnesium alloys have comparatively lower mechanical properties and wear resistance [4]. The wear limitation of magnesium can be improved by adding ceramic materials to the base metal [5]. Magnesium metal matrix composites have enhanced properties compared to magnesium alloys, like high stiffness, high specific strength, and also improved wear resistance [6, 7]. In general, silicon carbide particles are the most favorable reinforcement due to their high hardness and low cost [8]. The tensile and wear properties of composites are also effectively improved by using micro silicon carbide particles due to their easy dispersion during the manufacturing process [9, 10]. The addition of SiC to AZ91 up to 2%, increases the mechanical properties and thermal stability and decreases beyond 2% [11]. The decrease in ultimate tensile strength, and increase in yield strength and hardness is observed in AZ91 alloy SiC composite, with an increase in percentage of reinforcement [12, 13] and no interfacial reaction is observed at the interface of matrix and reinforcement [14]. From the above literature, it was found that the magnesium alloy composites with silicon carbide reinforcement of 3% or above exhibited excellent mechanical properties. The influence of control

*CONTACT: K.C.K. Kumar, e-mail: kchkk9874@gmail.com

parameters on wear and coefficient of friction for magnesium-based composite is predicted using Taguchi, analysis of variance (ANOVA), and regression analysis [15-18]. The Artificial Neural Network (ANN) models are used for the prediction of optimization of die casting parameters of AZ91D alloy and also discussed the higher efficiency of ANN model on prediction of significant factors [19]. The optimization of machining parameters using simulated annealing and pattern search is addressed [20]. The methodology for the ant lion optimization algorithm was proposed [21]. The optimization of wear for the aluminum alloy with SiC-Gr reinforcements was discussed by using the antlion algorithm [22]. A multi-objective optimization algorithm for solving engineering problems by using an Ant lion optimizing algorithm was reported [23]. Optimization of AZ31-SiC Composite using a whale optimization algorithm, particle swarm optimization, and fire fly algorithm [24]. Few attempts have been made to forecast magnesium-based composites' wear and coefficient of friction. Still, a considerable amount of ambiguity exists in the prediction of wear parameters using computational methods. Hence, the focus is made on this present work on the ANN modeling with single and multi-layer to predict the wear and coefficient of friction for AZ31 magnesium alloy SiC composite.

The present study is to investigate a well-trained network is expected to be a helpful and powerful tool for neural network modeling to predict the wear and COF of AZ31-SiC metal matrix composite. The rest of the paper is followed as the second section describes the experimental procedure and the third section presents experimental results. The fourth section presents the simulation results of ANN modeling with single and multi-hidden layer perception. The fifth section depicts the confirmation of experiments. The conclusion part is described in the sixth section.

## 2. MATERIALS AND METHODS

### 2.1 Materials and Manufacturing of Composites

Composites are fabricated by using the stir casting method. The AZ31 material was loaded into a graphite crucible and heated to a temperature of 750$^0$C to form a pool. An argon gas environment is provided during heating to avoid oxidation. The formation of the vortex was done by a stirrer with a graphite impeller rotating at a speed of 700 rpm and the addition of SiC reinforcement was done to have a uniform distribution. The liquid metal was dispensed into a preheated mold, and the homogenization process was done. The properties of AZ31 magnesium alloy reinforced with SiC at 1%, 2%, 3%, and 4% are tabulated in Table 1. The focus is made on AZ31- 4%SiC composite for the analysis due to its enhanced properties [25] presented in Table 1.

**Table 1.** Properties of AZ31-SiC composites

| Description | 0% | 1% | 2% | 3% | 4% |
|---|---|---|---|---|---|
| Density (kg/m$^3$) | 1.8 | 1.811 | 1.812 | 1.825 | 1.833 |
| Hardness (HRC) | 69.56 | 70.25 | 80.97 | 92.5 | 98.89 |
| Y.S. (MPa) | 65.09 | 72.05 | 86.31 | 92.6 | 88.44 |
| U.T.S (MPa) | 102.3 | 114.5 | 128.1 | 178.4 | 170.7 |
| Comp.Strength (MPa) | 173.4 | 194.3 | 313.3 | 365.5 | 380.2 |

### 2.2 Wear Test Experimentation

The ASTM G-99 standard composite specimens of AZ31-SiC are used for conducting experiments on a wear testing machine (Ducom) to determine the tribological properties. The composite pins of 8 mm diameter and 35 mm length are polished with 1200 grit of abrasive and are pressed against the counter body of the EN31 steel disc. The applied load is 50 N, the area of the pin in contact is 50.24 mm$^{2,}$ and the normal pressure acting on the pin is 0.995 MPa. The EN31 steel disc is harder than the developed composites, which is supposed to be a dominating factor for forecasting tribological behavior. The steel disc and pin are cleaned with acetone before each wear test to avoid the presence of non-desirable deposits. The wear tests were conducted for various control parameters of load (10, 15, and 20 N), velocity (0.5, 1, and 1.5 m/s), and sliding distance (500, 750, and 1000 m) with a full factorial design of experiments. The mass loss of the composite was calculated with a micro-weighing machine for each wear test. The wear rate (mg) of the composite is determined by the weight loss of the pin divided by the sliding distance. Taguchi, ANOVA, and Regression analysis were carried out for the wear results [26, 27]. The wear test data is used to form ANN sets as testing data(20%) and training data(80%). ANN modeling with single and multi hidden layer techniques is used for the prediction of wear and COF for various operating conditions.

### 2.3 ANN Modeling of Tribological Parameters Optimization

Artificial Neural Network is a mathematical modeling technique used to correlate the experimental data that are difficult to simulate with conventional models [28-30]. ANN is successfully utilized by researchers for predicting the optimum physical, mechanical, and wear properties [31]. The ANN model consists of three layers which are an input layer, a hidden layer, and an output layer. In this present work, 27 experimental data are divided into experiments data of 21 and training experiments data of 6. Among the 6 experiment data, ANN splits into three groups: Training (60%), independent testing (20%), and validation (20%). For the validation of the trained network, the testing set of 6 data was used. In the process of prediction of wear for the composite, modeling of the network is carried out with the variation of training function, transfer function, number of layers, and number of neurons. A prime flow chart is used to follow single and multi hidden layers for modeling is presented in Fig. 1.

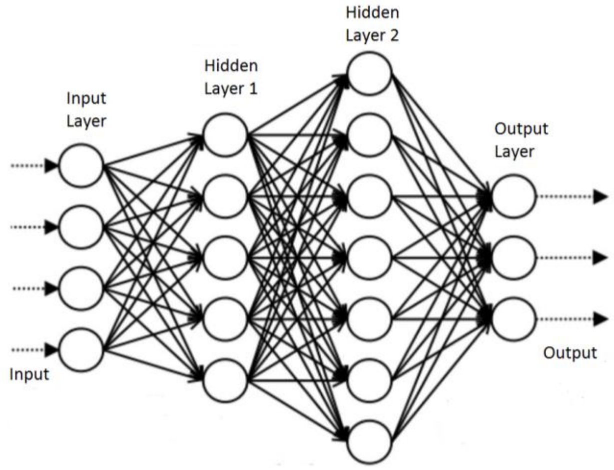


**Fig. 1.** ANN architecture

The ANN model with back propagation learning algorithm was more popular in recent time and is specifically used for engineering applications [32]. In this work, the ANN have been modeled with Feed Forward Back Propagation (FFBP) and Cascade Forward Back Propagation (CFBP) networks and Layer Recurrent (LR) networks with the selection of neurons and layers by trial and error method. Accordingly the ANN structure was optimized to identify the best process parameters for wear test [33] is shown in Fig. 2.

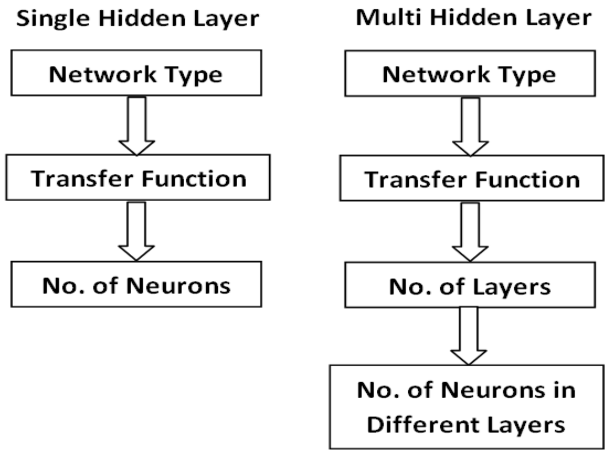


**Fig. 2.** Optimization flow chart for SHL and MHL

## 3. RESULTS AND DISCUSSIONS

### 3.1 Tribological Performance Charecterisitcs of AZ31/SiC composite

The wear test experiments for wear and COF for various loading conditions of load, speed, and sliding distance were conducted based on the full factorial design of experiments, and the results are presented in Table 2. The experimental investigation of the composite demonstrates that the minimum wear is noticed at a load of 10 N. The wear increases with the load increases due to deep penetration resulting in a higher material removal rate depicted in Fig. 3. The wear is proportional to the sliding distance, load, and inversely with the velocity. The influence of the load, speed, and sliding distance on wear and COF is analyzed using MINITAB software. This analysis is done for wear and COF separately using MINITAB software. ANOVA is used to study the effect of discrete process factors. The ANOVA analysis was employed at a confidence interval of 0.95 or a p-value of 0.05. It implies that the p-value resulting from any parameter ≤ 0.05 is significant. The conformity of the significance of individual parameters was accomplished with the aid of the main effects plot.

**Table 2.** Design of experiments using $L_{27}$ orthogonal array

| S. No | Load (N) | Velocity (m/s) | Distance (m) | Wear (mg) | COF |
|---|---|---|---|---|---|
| 1 | 10 | 0.5 | 500 | 4.053 | 0.390 |
| 2 | 10 | 0.5 | 750 | 4.514 | 0.470 |
| 3 | 10 | 0.5 | 1000 | 5.803 | 0.480 |
| 4 | 10 | 1 | 500 | 3.777 | 0.380 |
| 5 | 10 | 1 | 750 | 4.237 | 0.420 |
| 6 | 10 | 1 | 1000 | 4.974 | 0.450 |

**Table 2.** Design of experiments using $L_{27}$ orthogonal array - *Continuation of the Table from the previous page*

| | | | | | |
|---|---|---|---|---|---|
| 7 | 10 | 1.5 | 500 | 3.961 | 0.330 |
| 8 | 10 | 1.5 | 750 | 3.869 | 0.390 |
| 9 | 10 | 1.5 | 1000 | 5.159 | 0.460 |
| 10 | 15 | 0.5 | 500 | 4.974 | 0.467 |
| 11 | 15 | 0.5 | 750 | 5.896 | 0.493 |
| 12 | 15 | 0.5 | 1000 | 6.356 | 0.473 |
| 13 | 15 | 1 | 500 | 4.882 | 0.440 |
| 14 | 15 | 1 | 750 | 5.619 | 0.460 |
| 15 | 15 | 1 | 1000 | 5.896 | 0.487 |
| 16 | 15 | 1.5 | 500 | 4.698 | 0.433 |
| 17 | 15 | 1.5 | 750 | 4.974 | 0.453 |
| 18 | 15 | 1.5 | 1000 | 5.619 | 0.473 |
| 19 | 20 | 0.5 | 500 | 5.435 | 0.490 |
| 20 | 20 | 0.5 | 750 | 5.988 | 0.510 |
| 21 | 20 | 0.5 | 1000 | 7.185 | 0.530 |
| 22 | 20 | 1 | 500 | 4.974 | 0.470 |
| 23 | 20 | 1 | 750 | 5.435 | 0.495 |
| 24 | 20 | 1 | 1000 | 6.54 | 0.505 |
| 25 | 20 | 1.5 | 500 | 4.514 | 0.485 |
| 26 | 20 | 1.5 | 750 | 4.882 | 0.465 |
| 27 | 20 | 1.5 | 1000 | 6.264 | 0.490 |

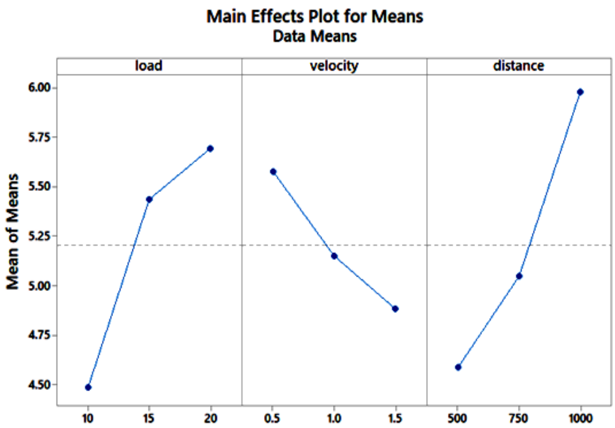


**Fig. 3**. Main effects plot for data means of wear

The ANOVA results obtained for wear and COF are presented in Table 3. These results reveal that the highest contributing parameter for wear is the distance of 45.72%, followed by a load of 36.83% and 11.21% of velocity and the highest contributing parameter for COF is the distance of 52.13%, followed by a load of 27.52% and 9.41% of velocity [28,29].

The regression equation for wear is obtained for the corresponding R, and R-Adjusted values of 94.18% and 92.43%, and for COF is obtained for the corresponding R and R-Adjusted values of 89.03% and 86.74%. The obtained regression equations are shown in Eq 1 and 2 [30]. The R-coefficient values are close to each other, which indicates that the relations between experimental parameters were well predicted and are significant. The values of interaction terms and higher-order terms are close to zero, and hence the model becomes linear.

$$\text{Wear} = 1.999 + 0.1208\,L - 0.696\,V + 0.002784\,D \quad (1)$$

$$\text{COF} = 0.3060 + 0.007444\,L - 0.03600V + 0.000103\,D \quad (2)$$

**Table 3.** ANOVA results for wear and COF

| Source | DF | SS | MS | F | P-Value | % of Contri-bution |
|---|---|---|---|---|---|---|
| **Wear** | | | | | | |
| Load | 2 | 0.2925 | 0.1462 | 67.82 | 0.00 | 39.4 |
| Velocity | 2 | 0.0774 | 0.0387 | 17.96 | 0.00 | 10.4 |
| Distance | 2 | 0.3277 | 0.1638 | 75.97 | 0.00 | 44.2 |
| Error | 20 | 0.0431 | 0.0021 | | | 5.8 |
| Total | 26 | 0.7409 | | | | 100 |
| **COF** | | | | | | |
| Load | 2 | 0.0219 | 0.0109 | 48.07 | 0.00 | 52.5 |
| Velocity | 2 | 0.0058 | 0.0029 | 12.76 | 0.00 | 13.9 |
| Distance | 2 | 0.0094 | 0.0047 | 20.68 | 0.00 | 22.6 |
| Error | 20 | 0.0045 | 0.0002 | | | 10.93 |
| Total | 26 | 0.0417 | | | | 100 |

## 3.2 Simulation results of ANN modeling

### *3.2.1 Simulation results of ANN modeling with Single Hidden Layer Perception*

The data set for Networks 1 to 18 framed with various inputs are tabulated in Table 4. The training function is considered as Trlm (Trainlm Transfer Function) for all the considered networks. The Network with the least error for wear and coefficient of friction is considered optimal. Purelin Transfer Function (Prln) transfer function exhibits a better error than Tan-Sigmoid and Log-Sigmoid as shown in Fig. 4. The next step is to optimize the type of network and number of neurons by fixing the transfer function as Prln. The data set for Networks 19 to 36 for wear and coefficient of friction are also tabulated in Table 4. The variation in the error from the networks 19-36, reveals that the CFBP network with 9 numbers neurons exhibited minimum error shown in Fig. 5. Hence, network number 2 was considered the best network for a single layer for wear and coefficient of friction with an error of ±6.10% and ±5.75%.

**Table 4.** Optimization of network type and number of layers

| Run | Network | Neurons | Transfer function | Wear Error (%) | COF Error (%) |
|---|---|---|---|---|---|
| 1 | CFBP | 9 | Logs | 13.43 | 13.20 |
| 2 | CFBP | 9 | Prln | 6.10 | 5.75 |
| 3 | CFBP | 9 | Trsg | 38.29 | 7.38 |
| 4 | FFBP | 9 | Logs | 6.64 | 8.77 |
| 5 | FFBP | 9 | Prln | 9.71 | 7.15 |
| 6 | FFBP | 9 | Trsg | 41.70 | 13.46 |
| 7 | LR | 9 | Logs | 15.07 | 6.94 |
| 8 | LR | 9 | Prln | 9.07 | 7.51 |
| 9 | LR | 9 | Trsg | 32.40 | 6.39 |
| 10 | CFBP | 10 | Logs | 21.57 | 9.28 |
| 11 | CFBP | 10 | Prln | 10.10 | 6.21 |
| 12 | CFBP | 10 | Trsg | 29.77 | 6.38 |
| 13 | FFBP | 10 | Logs | 6.46 | 14.37 |
| 14 | FFBP | 10 | Prln | 10.64 | 7.32 |
| 15 | FFBP | 10 | Trsg | 27.87 | 10.88 |
| 16 | LR | 10 | Logs | 12.92 | 6.17 |
| 17 | LR | 10 | Prln | 9.09 | 6.92 |
| 18 | LR | 10 | Trsg | 42.37 | 7.21 |
| 19 | CFBP | 7 | Prln | 8.372 | 6.386 |
| 20 | CFBP | 8 | Prln | 7.836 | 8.034 |
| 21 | CFBP | 9 | Prln | 6.109 | 5.757 |
| 22 | CFBP | 10 | Prln | 8.106 | 7.216 |
| 23 | CFBP | 11 | Prln | 8.391 | 6.781 |
| 24 | CFBP | 12 | Prln | 8.854 | 7.318 |
| 25 | FFBP | 7 | Prln | 11.28 | 9.675 |
| 26 | FFBP | 8 | Prln | 11.61 | 9.649 |
| 27 | FFBP | 9 | Prln | 9.710 | 7.151 |
| 28 | FFBP | 10 | Prln | 10.64 | 9.322 |
| 29 | FFBP | 11 | Prln | 8.789 | 7.585 |
| 30 | FFBP | 12 | Prln | 8.582 | 7.526 |
| 31 | LR | 7 | Prln | 10.01 | 10.09 |
| 32 | LR | 8 | Prln | 8.784 | 11.51 |
| 33 | LR | 9 | Prln | 9.076 | 7.517 |
| 34 | LR | 10 | Prln | 9.09 | 10.92 |
| 35 | LR | 11 | Prln | 9.062 | 8.900 |
| 36 | LR | 12 | Prln | 9.753 | 10.49 |

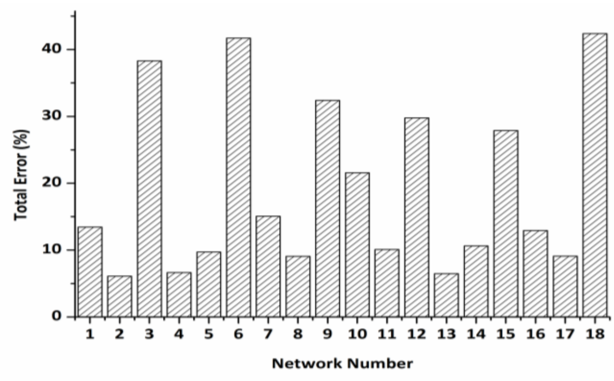


**Fig. 4.** Error (%) for SHL-ANN architecture (Network Nos. 1−18) for Wear

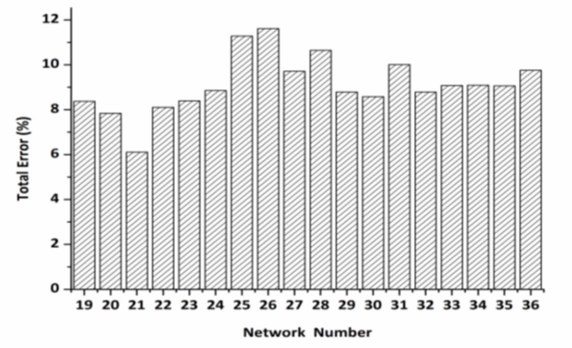


**Fig. 5.** Error (%) for SHL-ANN architecture (Network Nos. 19−36) for Wear

The best validation image for network number 2 is presented in Fig. 6, and the corresponding regression plots are also presented in Fig. 7. The dashed line represents the best linear fit. The regression plots indicate the training errors, test errors, and validation errors. As most of the data points were close to the central line, the model was considered accurate. The confirmation of predicted and test results are closer with an overall correlation coefficient of 0.982 as shown in Fig.7 [34].

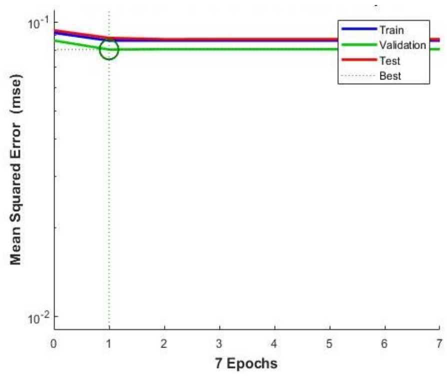


**Fig. 6.** Performance plot of optimized Network (No: 2) for SHL-ANN architecture

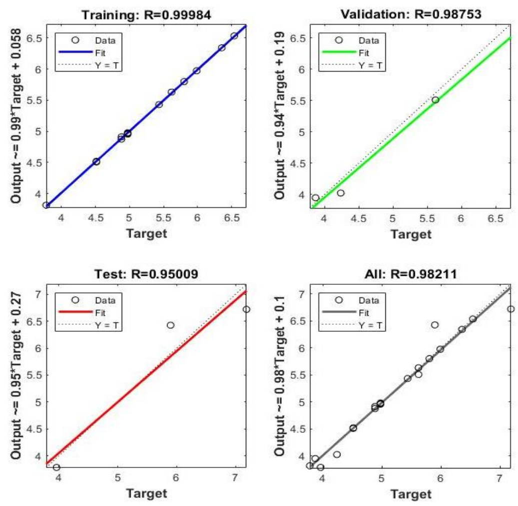


**Fig. 7.** Regression plot of optimized Network (No: 2) for SHL-ANN architecture

### 3.2.2 Simulation results of ANN modeling with Multi Hidden Layer perception

Multi-layered network was executed for the improvement of the accuracy of predicted results. The multi hidden layer network architecture was primarily built with 2, 3, and 4 hidden layers with Trlm and Prln as the functions. The multi-layered data set with 9 number of neurons for Networks 37 to 45 is tabulated in Table 5. The corresponding error is presented in Fig. 8. The FFBP network with three layers is considered accurate from the data of networks 37 to 45. In order to find the optimum parameters in multi multi-layered network, networks 46 to 66 are considered and corresponding errors are tabulated in Table 5.

**Table 5.** Optimization of network type and number of layers (Network 37-45)

| Run | Network | No. of Layers | Neurons | Wear Error (%) | COF Error (%) |
|---|---|---|---|---|---|
| 37 | *CFBP* | 2 | 9, 9 | 7.752 | 7.423 |
| 38 | *CFBP* | 3 | 9, 9, 9 | 9.299 | 5.881 |
| 39 | *CFBP* | 4 | 9, 9, 9, 9 | 10.07 | 6.825 |
| 40 | *FFBP* | 2 | 9, 9 | 12.25 | 6.512 |
| 41 | *FFBP* | 3 | 9, 9, 9 | 9.844 | 5.477 |
| 42 | *FFBP* | 4 | 9, 9, 9, 9 | 8.215 | 6.035 |
| 43 | *LR* | 2 | 9, 9 | 11.79 | 6.630 |
| 44 | *LR* | 3 | 9, 9, 9 | 8.995 | 5.484 |
| 45 | *LR* | 4 | 9, 9, 9, 9 | 8.910 | 6.962 |
| 46 | *FFBP* | 3 | 9, 9, 1 | 7.924 | 6.903 |
| 47 | *FFBP* | 3 | 9, 9, 3 | 11.691 | 7.600 |
| 48 | *FFBP* | 3 | 9, 9, 5 | 8.530 | 8.088 |
| 49 | *FFBP* | 3 | 9, 9, 7 | 10.326 | 7.587 |
| 50 | *FFBP* | 3 | 9, 9, 9 | 9.177 | 7.175 |
| 51 | *FFBP* | 3 | 9, 9, 11 | 8.685 | 7.032 |
| 52 | *FFBP* | 3 | 9, 9, 13 | 9.594 | 6.740 |
| 53 | *FFBP* | 3 | 9, 1, 9 | 7.481 | 5.933 |
| 54 | *FFBP* | 3 | 9, 3, 9 | 7.178 | 6.564 |
| 55 | *FFBP* | 3 | 9, 5, 9 | 8.624 | 6.734 |
| 56 | *FFBP* | 3 | 9, 7, 9 | 9.087 | 6.432 |
| 57 | *FFBP* | 3 | 9, 9, 9 | 8.427 | 5.947 |
| 58 | *FFBP* | 3 | 9, 11, 9 | 7.911 | 6.286 |
| 59 | *FFBP* | 3 | 9, 13, 9 | 8.962 | 7.425 |
| 60 | *FFBP* | 3 | 1, 9, 9 | 10.790 | 6.263 |
| 61 | *FFBP* | 3 | 3, 9, 9 | 8.342 | 6.391 |
| 62 | *FFBP* | 3 | 5, 9, 9 | 12.901 | 7.548 |
| 63 | *FFBP* | 3 | 7, 9, 9 | 6.777 | 5.526 |
| 64 | *FFBP* | 3 | 9, 9, 9 | 8.147 | 6.763 |
| 65 | *FFBP* | 3 | 11, 9, 9 | 9.883 | 8.632 |
| 66 | *FFBP* | 3 | 13, 9, 9 | 9.158 | 5.806 |

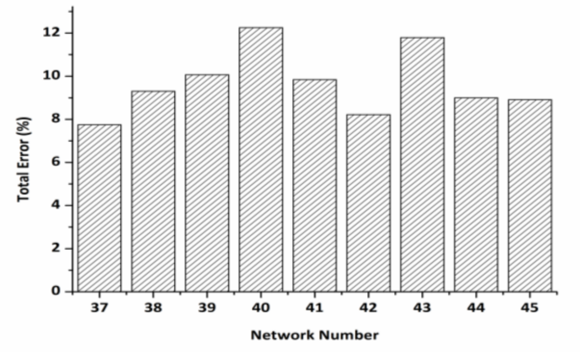


**Fig. 8.** Error (%) for MHL-ANN architecture (Network Nos. 37–45) for Wear

The errors for networks 46 to 66 are presented in Fig. 9, revealing that the network (63) with 7-9-9 neurons was considered better than others with an error of 6.777% for the wear rate and 5.526% for the coefficient of friction. Therefore, the FFBP network with Prln transfer functions and 7-9-9 neurons is considered to be optimum. The best validation image for the network number 63 is presented in Fig. 10, and the corresponding regression plots are also presented in Fig. 11. The dashed line represents the best linear fit. The regression plots indicate the training errors, test errors, and validation errors. As most of the data points were close to the central line, the model was considered accurate. The confirmation of - predicted and test results are closer with an overall correlation coefficient of 0.943 [35].

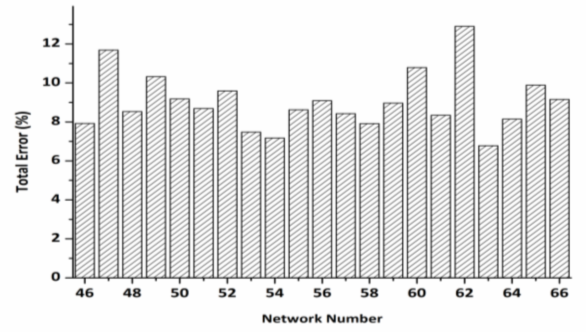


**Fig. 9.** Error (%) for MHL-ANN architecture (Network Nos. 46–66) for Wear

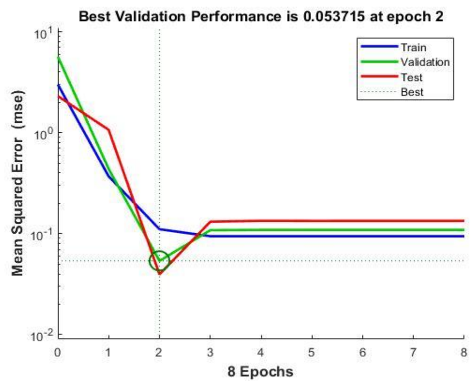


**Fig. 10.** Performance plot of optimized Network (No: 63) for MHL-ANN architecture

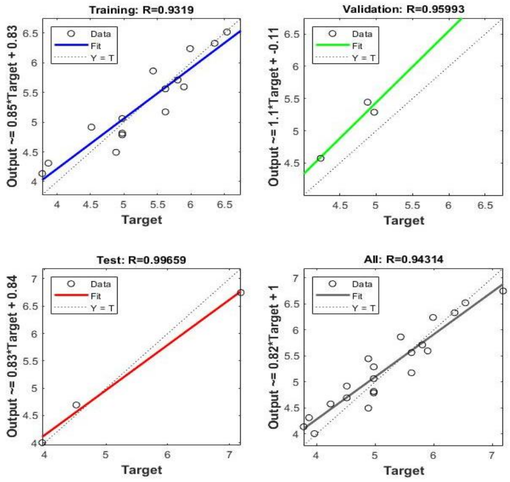


**Fig. 11.** Regression plot of optimized Network (No: 63) for MHL-ANN architecture

The optimized networks of ANN modeling with single and multi hidden layer perception are tabulated in Table 6. Trlm and Prln act as training and transfer functions to predict better results in both single and multi hidden layer perception [36]. The ANN model delivers the CFBP network with single hidden layer perception and the FFBP network with multi hidden layer for the prediction of better results for wear and COF.

**Table 6.** Best predicted network in SHL-ANN and MHL-ANN architectures with Trlm as Train Function

| Network | Layers | Neurons | Transfer function | Wear | COF |
|---|---|---|---|---|---|
| | | | | Total Error (%) | Total Error (%) |
| CFBP | 1 | 9 | Prln | 6.10 | 5.75 |
| FFBP | 3 | 7, 9, 9 | Prln | 6.777 | 5.526 |

### *3.2.3 Confirmation of experiments*

In the last stage of the design of the experiment i.e., confirmation test, execution of a specific combination of the process parameters for wear and COF is carried out for validation. The output results for a set of control parameters from the experiments are compared with the results of regression analysis and with the results of ANN modeling with single and multi hidden layers. These comparison results are tabulated for wear and coefficient of friction in Table 7. The deviation error for the values from regression analysis and ANN are calculated as the percentage of deviation and the range of deviation is less than 9%. The results from ANN modeling with multi-layer are closer to the experimental values. Hence ANN models were confirmed as precise.

**Table 7.** Confirmatory tests for the wear and COF

| **Wear** | | | | | | | | | |
|---|---|---|---|---|---|---|---|---|---|
| Load (L) | Velocity (V) | Distance (D) | Experimental Results Wear (mg) | Prediction | | | | | |
| | | | | Regression | | Single hidden layer | | Multi hidden layer | |
| | | | | Predicted Results | Deviation (%) | Predicted Results | Deviation (%) | Predicted Results | Deviation (%) |
| 10 | 0.7 | 600 | 4.3902 | 4.075 | 7.17 | 4.1832 | 4.71 | 4.2095 | 4.11 |
| 15 | 0.9 | 800 | 5.4118 | 5.328 | 1.54 | 5.3862 | 0.47 | 5.3926 | 0.35 |
| 20 | 1.2 | 900 | 6.213 | 6.0854 | 2.05 | 6.1321 | 1.30 | 6.0640 | 0.88 |
| 20 | 1.4 | 1000 | 6.2246 | 6.172 | 0.84 | 6.1953 | 0.47 | 6.2075 | 0.27 |
| **COF** | | | | | | | | | |
| Load (L) (N) | Velocity (V) (m/s) | Distance (D) (m) | Experimental Results COF | Prediction | | | | | |
| | | | | Regression | | Single hidden layer | | Multi hidden layer | |
| | | | | Predicted Results | Deviation (%) | Predicted Results | Deviation (%) | Predicted Results | Deviation (%) |
| 10 | 0.7 | 600 | 0.442 | 0.417 | 5.65 | 0.4192 | 5.15 | 0.4219 | 4.54 |
| 15 | 0.9 | 800 | 0.465 | 0.4526 | 2.66 | 0.4558 | 1.97 | 0.4611 | 0.83 |
| 20 | 1.2 | 900 | 0.495 | 0.4761 | 3.81 | 0.4891 | 1.19 | 0.4923 | 0.54 |
| 20 | 1.4 | 1000 | 0.487 | 0.4433 | 8.97 | 0.4588 | 5.79 | 0.4681 | 3.88 |

## 4. CONCLUSIONS

In this present work, the modeling of tribological properties of AZ31-SiC composite using the ANN fabricated through the stir casting method was done. AZ31-SiC metal matrix composite was fabricated through a stir-casting process. The twenty-seven tests were performed with three types of loads, sliding speeds, and sliding distances on the wear testing machine for the formation of training sets of ANN. Using the output data of the wear tests, Taguchi, analysis of variance (ANOVA), and regression analysis were carried out to determine the effect of the control parameters on the wear and COF. The results from ANN modeling prove its practicability and fine correlation with the experimental results. The following conclusions were emerging from the present study:

1. Taguchi analysis depicts that the wear and coefficient of friction increase with an increase in load, and decrease in distance, with an increase in sliding velocity.
2. ANOVA depicts that distance is the highest contributor followed by load and sliding velocity for wear and load is the highest contributor followed by distance and sliding velocity for COF.
3. Regression analysis equations were developed for the prediction of wear and COF.
4. An alternative method of ANN modeling can be used for the prediction of tribological parameters without conducting the wear test which saves a lot of time, and cost.
5. In the ANN model with single hidden layer perception, the Cascade Forward Back Propagation (CFBP) network with Trlm and Prln as the functions provides the best prediction results with an optimum percentage of error of 6.1%, 5.75% for wear and COF respectively.
6. In the ANN model with multi hidden layer perception, Feed Forward Back Propagation (FFBP) network with Trlm and Prln as the functions provides the best prediction results with an optimum percentage of error of 6.777%, and 5.52% for wear and COF respectively.
7. The maximum percentage of deviation in ANN modeling with single and multi hidden layers is less than 9%. Hence ANN modeling may be used as an alternative method for the prediction of wear and COF for optimization of tribological parameters. This prediction process saves time and effort for experimentation.

## NOMENCLATURE:

***CFBP*** *:* Cascade Forward Back Propagation, ***FFBP*** *:* Feed Forward Back Propagation, ***LR*** *:* Layer Recurrent, ***Trlm*** *:* Trainlm Transfer Function, ***Prln*** *:* Purelin Transfer Function, ***Trsg*** *:* Transig Transfer Function, ***Logs*** *:* Logsig Transfer Function.

## REFERENCES


[1] Y. Huang, Q. Ouyang, D. Zhang, J. Zhu, R. Li, H. Yu, Carbon Materials Reinforced Aluminum Composites: A Review. *Acta Metallurgica Sinica,* 27, 2014: 775-786. https://doi.org/10.1007/s40195-014-0160-1

[2] A. Vencl, N.M. Vaxevanidis, M. Kandeva, A bibliometric analysis of scientific research on tribology of composites in Southeastern Europe. *IOP Conference Series: Materials Science and Engineering*, 724, 2020: 012012. https://doi.org/10.1088/1757-899X/724/1/012012

[3] P.K. Kumar, N.V. Sai, A.G. Krishna, Effect of $Y_2O_3$ addition and cooling rate on mechanical properties of Fe-24Cr-20Ni-2Mn steels by powder metallurgy route. *Composite Communication*, 10, 2018: 116-121. https://doi.org/10.1016/j.coco.2018.09.003

[4] V. Sklenicka, M. Svoboda, M. Pahutova, K, Kucharova T.G. Langdon, Microstructural processes in creep of an AZ 91 magnesium-based composite and its matrix alloy. *Material Science and Engineering A*, 319-321, 2001: 741-745. https://doi.org/10.1016/S0921-5093(01)01023-1

[5] X.-l. Zhang, G.-k. Yu, W.-b. Zou, Y.-s. J, Y.-z. Liu, J.-l. Cheng, Effect of casting methods on microstructure and mechanical properties of ZM5 space flight magnesium alloy. *China Foundry*, 15, 2018: 418-421. https://doi.org/10.1007/s41230-018-8098-y

[6] S.-J. Huang, Y.-R. Jeng, V.I. Semenov, Y.-Z. Dai, Particle size effects of silicon carbide on wear behavior of SiC p-reinforced magnesium matrix composites. *Tribology Letters,* 42, 2011: 79-87. https://doi.org/10.1007/s11249-011-9751-4

[7] S.F. Hassan, N.O. Ogunlakin, N. Al-Aqeeli, S. Nouari, M.M.A. Baig, F. Patel, Development of tensile-compressive asymmetry free magnesium based composite using $TiO_2$

nanoparticles dispersion. *Journal* of *Materials Research*, 33, 2018: 130-137. https://doi.org/10.1557/jmr.2017.430

[8] M. Rashad, F. Pan, H. Hu, M. Asif, S. Hussain, J. She, Enhanced tensile properties of magnesium composites reinforced with grapheme nanoplatelets. *Materials Science Engineering A*, 630, 2015: 36-44. https://doi.org/10.1016/j.msea.2015.02.002

[9] S. Basavarajappa, G. Chandramohan, K. Mukund, M. Ashwin, M. Prabu, Dry Sliding Wear Behavior of Al 2219/SiCp-Gr Hybrid Metal Matrix Composites. *Journal of Materials Engineering and Performance*, 15, 2006: 668-674. https://doi.org/10.1361/105994906X150803

[10] Q.B. Nguyen, Y.H.M. Sim, M. Gupta, C.Y.H. Lim, Tribology characteristics of magnesium alloy AZ31B and its composites. *Tribology International,* 82(Part B), 2015: 464-471. https://doi.org/10.1016/j.triboint.2014.02.024

[11] S.-J. Huang, A. Negash Ali, Experimental investigations of effects of SiC contents and severe plastic deformation on the microstructure and mechanical properties of SiCp / AZ61 magnesium metal matrix composites. *Journal of Materials Processing Technology*, 272, 2019: 28-39. https://doi.org/10.1016/j.jmatprotec.2019.05.002

[12] K.K. Deng, K. Wu, Y.W. Wu, K.B. Nie, M.Y. Zheng, Effect of submicron size SiC particulates on microstructure and mechanical properties of AZ91 magnesium matrix composites. *Journal of alloys and compounds,* 504(2), 2010: 542-547. https://doi.org/10.1016/j.jallcom.2010.05.159

[13] K.B. Nie, X.J. Wang, K. Wu, X.S. Hu, M.Y. Zheng, L. Xu, Microstructure and tensile properties of micro-SiC particles reinforced magnesium matrix composites produced by semisolid stirring assisted ultrasonic vibration. *Materials Science and Engineering A*, 528(29-30), 2011: 8709-8714. https://doi.org/10.1016/j.msea.2011.08.035

[14] A. Asgari, M. Sedighi, P. Krajnik, Magnesium alloy-silicon carbide composite fabrication using chips Waste. *Journal of Cleaner Production*, 232, 2019: 1187-1194. https://doi.org/10.1016/j.jclepro.2019.06.018

[15] K.B. Nie, X.J. Wang, K. Wu, L. Xu, M.Y. Zheng, X.S. Hu, Fabrication of SiC particles-reinforced magnesium matrix composite by ultrasonic vibration. *Journal of Materials Science*, 47, 2012: 138-144. https://doi.org/10.1007/s10853-011-5780-5

[16] S. Sathish, V. Anandakrishnan, S. Sankaranarayanan, M. Gupta, Optimization of wear parameters of magnesium metal-metal composite using Taguchi and GA technique. *Journal Tribologi*, 23, 2019: 76-89. https://doi.org/10.1590/1980-5373-MR-2022-0467

[17] S.K. Khatkar, R. Verma, Sumankant, S.S. Kharb, A. Thakur, R. Sharma, Optimization and Effect of Reinforcements on the Sliding Wear Behavior of Self-Lubricating AZ91D-SiC-Gr Hybrid Composites. *Silicon*, 13, 2021: 1461-1473. https://doi.org/10.1007/s12633-020-00523-0

[18] C. Sankar, K. Gangatharan, S.C.E. Singh, R.K. Sharma, K. Mayandi, Optimization on Tribological Behaviour of Milled Nano-$B_4C$ Particles Reinforced with AZ91 Alloy Through Powder Metallurgy Method. *Transactions of Indian Institute of Metals*, 72, 2019: 1255-1275. https://doi.org/10.1007/s12666-019-01618-y

[19] B.M. Girish, B.M. Satish, S. Sarapure, Basawaraj, Optimization of Wear Behavior of Magnesium Alloy AZ91 Hybrid Composites Using Taguchi Experimental Design. *Metallurgical and Materials Transactions A*, 47, 2016: 3193-3200. https://doi.org/10.1007/s11661-016-3447-1

[20] S. Ghalme, A. Mankar, Y. Bhalerao, Integrated Taguchi-simulated annealing (SA) approach for analyzing wear behaviour of silicon nitride. *Journal of Applied Research and Technology,* 15(6), 2017: 624-632. https://doi.org/10.1016/j.jart.2017.08.003

[21] M.-C. Chen, D.-M. Tsai, A simulated annealing approach for optimization of multi-pass turning operations. *International Journal of Production and Research*, 34(10), 1996, 2803-2825. https://doi.org/10.1080/00207549608905060

[22] S. Mirjalili, The Ant Lion Optimizer. *Advances in Engineering Softwares,* 83, 2015: 80-98. https://doi.org/10.1016/j.advengsoft.2015.01.010

[23] A.G. Joshi, M. Manjaiah, S. Basavarajappa, R. Sures, Wear Performance Optimization of SiC-Gr Reinforced Al Hybrid Metal Matrix Composites Using Integrated Regression-Antlion Algorithm. *Silicon*, 13, 2021: 3941-3951.

https://doi.org/10.1007/s12633-020-00704-x

[24] K.C.K Kumar, B.R. Kumar, N.M. Rao, Tribological Parameters Optimization of AZ31-SiC Composite Using Whale Optimization Algorithm. *Journal of Materials Engineering and Performance,* 32, 2023: 2735-2748. https://doi.org/10.1007/s11665-022-07570-1

[25] K.C.K Kumar, B.R. Kumar, N.M. Rao, Microstructural, Mechanical Characterization, and Fractography of AZ31/SiC Reinforced Composites by Stir Casting Method. *Silicon*, 14 2022: 5017-5027. https://doi.org/10.1007/s12633-021-01180-7

[26] J.-Lian Wen, J.-R. Shie, Y.-K. Yang, Optimization of a Wear Property of Die Cast AZ91D Components via a Neural Network. *Materials and Manufacturing Processes*, 24(4), 2009: 400-408. https://doi.org/10.1080/10426910802714274

[27] D. Nayak, N. Ray, R. Sahoo, M. Debata, Analysis of Tribological Performance of Cu Hybrid Composites Reinforced with Graphite and TiC Using Factorial Techniques. *Tribology Transactions,* 57(5), 2014: 908-918. https://doi.org/10.1080/10402004.2014.923079

[28] M.O. Bodunrin, K.K. Alaneme, L.H. Chown, Aluminium matrix hybrid composites: A review of reinforcement philosophies; mechanical, corrosion and tribological *characteristics. Journal of Materials Research and Technology*, 4(4), 2015: 434-445. https://doi.org/10.1016/j.jmrt.2015.05.003

[29] N. Radhika, R. Subramaniam, Wear behaviour of aluminium/alumina/graphite hybrid metal matrix composites using Taguchi's techniques. *Industrial Lubrication and Tribology*, 65(3), 2013, 166-174. https://doi.org/10.1108/00368791311311169

[30] A.H.S. Rahiman, D.S.R. Smart, B. Wilson, I. Ebrahim, B. Eldhose, B. Mathew, R.T. Murickan, Dry sliding wear analysis OF Al5083/CNT/Ni/MoB hybrid composite using DOE Taguchi method. *Wear,* 460-461, 2020: 203471. https://doi.org/10.1016/j.wear.2020.203471

[31] S. Veličković, B. Stojanović, M. Babić, I. Bobić, Optimization of tribological properties of aluminum hybrid composites using Taguchi design. *Journal of Composite Materials*, 51(17), 2017: 1-11. https://doi.org/10.1177/0021998316672294

[32] S.D. Saravanan, M. Senthilkumar, Prediction of tribological behaviour of rice husk ash reinforced aluminum alloy matrix composites using artificial neural network. *Russian Journal of Non-Ferreous Metals,* 56, 2015: 97-106. https://doi.org/10.3103/S1067821215010174

[33] A. Fathy, AA. Megahed, Prediction of abrasive wear rate of in situ Cu–$Al_2O_3$ nanocomposite using artificial neural networks. *The International Journal of Advances Manufacturing Technology*, 62, 2012: 953-963. https://doi.org/10.1007/s00170-011-3861-x

[34] Z.Y. Jiang, Z. Zhang, K. Friedrich, Prediction on wear properties of polymer composites with artificial neural networks. *Composites Science and Technology*, 67(2), 2007: 168-176. https://doi.org/10.1016/j.compscitech.2006.07.026

[35] R. Egala, G.V. Jagadeesh, S.G. Setti, Experimental investigation and prediction of tribological behavior of unidirectional short castor oil fiber reinforced epoxy composites. *Friction*, 9, 2019, 250-272. https://doi.org/10.1007/s40544-019-0332-0

[36] F. Alambeigi, S.M. Khadem, H. Khorsand, E.M.S. Hasan, A comparison of performance of artificial intelligence methods in prediction of dry sliding wear behaviour. *The International Journal of Advances Manufacturing Technology,* 84, 2016: 1981-1994. https://doi.org/10.1007/s00170-015-7812-9